Simulating arbitrary interactions between small-scale space debris and a space-based pulsed laser system

Pieters, Liam; Noomen, Ron

DOI
10.1016/j.asr.2022.04.049

Publication date
2022

Document Version
Final published version

Published in
Advances in Space Research

Citation (APA)
Pieters, L., & Noomen, R. (2022). Simulating arbitrary interactions between small-scale space debris and a space-based pulsed laser system. *Advances in Space Research*, *72*(7), 2778-2785. https://doi.org/10.1016/j.asr.2022.04.049

Available online at www.sciencedirect.com

ScienceDirect

Advances in Space Research 72 (2023) 2778–2785

ADVANCES IN SPACE RESEARCH (a COSPAR publication)

www.elsevier.com/locate/asr

Simulating arbitrary interactions between small-scale space debris and a space-based pulsed laser system

Liam Pieters *, Ron Noomen

TU Delft, Faculty of Aerospace Engineering, Kluyverweg 1, 2629HS Delft, the Netherlands

Received 22 December 2021; received in revised form 10 March 2022; accepted 21 April 2022
Available online 27 April 2022

Abstract

This research investigates the performance of a space-based laser system to remove debris objects with size smaller than 10 cm. The laser system is placed in a 800 km Sun Synchronous Orbit and consists of a 20 kW laser that shoots 300 J energy pulses with a repetition frequency of 66.66 Hz. The system is able to detect and track debris objects in situ using a 2.0 m mirror from 800 km distance. From a distance of about 500 km, the laser fluence on the targets is sufficiently high to trigger ablation, which decelerates the debris objects and reduces their lifetime. The feasibility of the concept is tested in scenarios where the laser system targets the debris objects from a different orbiting altitude and from varying azimuth angles. For many geometries, the laser is capable of significantly reducing the lifetime of the debris object. Extrapolating to longer periods of operation, the laser can be expected to provide a significant reduction of the population of small debris objects in LEO.

Keywords: Active Debris Removal; space debris; laser debris removal; ablation; Low Earth Orbit

1. Introduction

Every launch of any space mission generates debris in space. A method for waste-removal in space has never been set in place, resulting in the current scenario where an estimated 900,000 debris fragments larger than 1 cm are orbiting Earth, of which every single one poses a serious danger for active satellites (Krag, 2020). A specifically difficult subpopulation is found in debris fragments with sizes between 1 and 10 cm, which are large enough to potentially break up a spacecraft in a collision, but are too small to monitor (Klinkrad, 2006). Reducing this subset of objects is paramount for a safe future of spaceflight.

Here we investigate the performance and feasibility of a space-based laser system acting on the LEO debris population. It is currently the only plausible technique to remove debris fragments below 10 cm since it monitors debris objects 'in situ' and autonomously, does not require contact with the debris objects, and can target objects in a continuous fashion when powered by solar panels. A ground-based laser system would not work for this purpose: objects with sizes below 10 cm are too small to track from Earth. Debris mitigation using just momentum transfer of photon pressure of an in-orbit laser system has also been studied, but was found to be less effective than an ablative system (Walker et al., 2021; Walker and Vasile, 2021).

The approach to lower debris objects using space-based laser ablation was first brought forward in 1991 (Schall, 1991). In many ways, the design is still the same in current proposals: an in-orbit satellite equipped with a laser and optics to ablate an object and a subsystem that controls the detection target acquisition. Various adaptations of a space-based laser have since then been proposed. This paper intends to contribute to the literature on orbital laser

* Corresponding author.
E-mail addresses: Liampieters@gmail.com (L. Pieters), r.noomen@tudelft.nl (R. Noomen).

https://doi.org/10.1016/j.asr.2022.04.049
0273-1177/

systems: how does a hypothetical laser perform in LEO, taking into account the exact (and changing) orbital geometry of the objects? The aim of this paper is to express the potential of space-based laser debris removal and to encourage further research on the subject.

2. Methodology

The laser is tested on debris objects in various orbital geometries. After each encounter, the reduced lifetime of the target is computed and compared to its nominal lifetime to assess the effects of the laser interaction.

2.1. Target acquisition

The space-based laser system will track debris objects longitudinally as it encounters them in orbit. The design of the subsystem for target acquisition and tracking is adopted from (Phipps and Bonnal, 2016). This paper intends to expand on that research by checking the ablative performance of the laser system in different scenarios. For completeness, the workings are briefly explained: the subsystem consists of two telescopes. One static large 60° Field-of-View (FOV) telescope will passively detect the reflected sunlight of potential debris objects. A second smaller active telescope with a 6 mrad FOV telescope will be pointed to the debris object and send low 1 Joule pulses, which will reflect a much higher Signal to Background Ratio (SBR) than the reflected sunlight. These high SBR pulses will let the system measure the distance in order for the laser to focus, after which the energy in the pulse can be increased until ablation is achieved. The smaller telescope will be the only component that will be actively steered. In this configuration, the laser only acquires objects that are moving towards it within a FOV of 60°.

2.2. Ablation

Ablation is achieved when the laser beam energy density at the target (the so-called fluence) exceeds a certain threshold, specific for the target material. The fluence is defined as follows (Phipps, 2014):

$$\Phi = \frac{4 \cdot E_{pulse} \cdot D_{eff}^2}{\pi \cdot M^4 \cdot a^2 \cdot \lambda^2 \cdot L^2} \tag{1}$$

in which E_{pulse} is the laser energy pulse. Other parameters are the laser beam quality M^2, the laser wavelength λ, the propagation distance L, the diffraction constant a and the effective mirror diameter D_{eff}.

With this, the exerted force on a target area can be described as (Mason et al., 2011):

$$F_{thrust} = \Phi_{eff} \cdot A_{target} \cdot C_m \cdot f \tag{2}$$

where A_{target} is the cross-sectional area of the object, C_m is an experimentally determined material-specific coefficient that shows how much power is converted to thrust, f is the pulse frequency and the relation $\Phi_{eff} = T_{eff} \cdot \Phi$is implemented, where T_{eff} accounts for system performance losses such as atmospheric disturbances or laser attenuation. The acceleration of the debris object is computed by dividing this force by its mass.

2.3. Laser parameters

Table 1 shows the parameters of the laser system. Special attention should be given to the material-specific coefficient C_m which greatly determines the efficiency of the interaction. A conservative value of 30N/MW is used here (Phipps and Boustie, 2017). Momentum transfer generated only through the effects of photon pressure is much less efficient. If the debris object would reflect all incoming laser photons, a maximum value for C_m can be achieved of $6.66 \cdot 10^{-3}$N/MW, which is around 3 orders of magnitude lower than when the debris object is ablated.

2.4. Propagation

A typical encounter will have the following steps: First, the orbits of the laser and debris object are initialised so that they will encounter each other with a certain geometry. The orbits are propagated with a stepsize of 10 s until the relative distance is below 800 km and the debris object can be 'detected'. The laser will focus its beam on the target and ablation is achieved at a distance of about 500 km. The laser interaction will stop when one of the following termination conditions is satisfied:

- $\mathbf{d}_{rel} \cdot \mathbf{v}_{rel} \geqslant 0$: the debris object has passed the laser.
- $\omega > 2^o/s$: during target tracking, the laser should not rotate faster than what the state-of-the-art attitude-control mechanisms can deliver (Phipps, 2014).

The first condition ensure that objects that are moving away from the laser are never targeted, since this would only increase the object's orbital energy. The orbits are propagated using a Runge–Kutta 4 model, which proved sufficiently accurate for the purposes of this study. The laser orbit and the debris objects are influenced by Earth's gravity, SRP, aerodynamic effects and luni-solar perturbations. The perturbation due to the laser interaction are implemented as in Fig. 1. The exerted force is split up in a normal, a radial component and a tangential component.

Table 1
Parameters of the laser system.

Parameter	Value	Parameter	Value
$P_{subsystems}$ [kW]	7	$C_{m,alu}$ [N/MW]	30
P_{laser} [kW]	20	A_{solar} [m^2]	100
E_{pulse} [J]	300	T_{eff}	0.9
f_{pulse} [Hz]	66.66	M^2	2.0
D_{eff} [m]	2.0	a	1.27
λ [nm]	335		

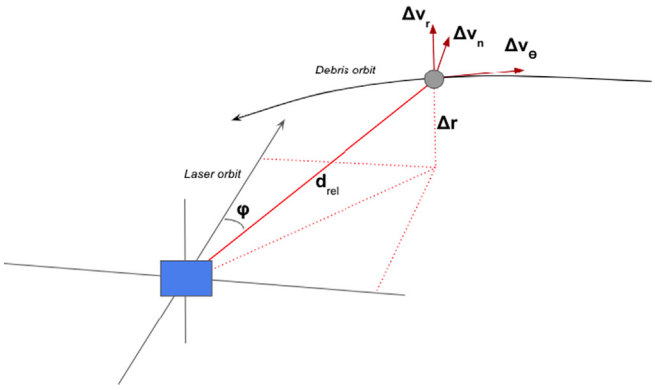

Fig. 1. Perturbing force due laser ablation split in three directions. Laser system interacts with debris object from azimuth angle ϕ and altitude difference Δr.

A force in the tangential component results in the most effective decrease in lifetime. Nevertheless, the components in the radial and normal component should also be inspected, as they can still result in a change in orbital parameters of the debris object.

The atmosphere is assumed to have an exponential profile with $\rho_0 = 2.51 \cdot 10^{-10}$ kg/m^3 and a scale height H of 82.0 km. The corresponding atmospheric densities are discussed in A.

2.5. Orbital lifetime

The main scope of this study is to compare the orbital lifetime of the debris objects before and after the laser interaction, so the lifetime computation is essential. To first order, the orbital lifetime of LEO objects can be assumed as follows (Wertz et al., 2011):

$$T_{life} = \frac{T_{period} \cdot H}{2\pi C_D (\frac{A}{m}) \rho a^2} \tag{3}$$

with T_{period} the time of one revolution at semi-major axis a, H the atmospheric scale height, ρ the atmospheric density at a, C_D the drag coefficient and (A/m) the Area-to-Mass Ratio (AMR) of the object.

Eq. 3 shows that the orbital lifetime of an object depends on its AMR. The AMR range for objects between 1 and 10 cm objects lies between 0.04 and 0.5 m^2/kg (Anz-Meador and Potter, 1996). Therefore, the laser system will be tested on three objects with different diameter and AMR: a 1 cm object with an AMR of 0.16 m^2/kg, a 5 cm object with an AMR of 0.07 m^2/kg and a 10 cm object with an AMR of 0.04 m^2/kg.

Since Eq. 3 only holds for circular orbits with constant atmospheric density throughout the orbit, an estimation has to be made for the average density throughout an elliptical orbit. This can be assumed to be the density at an effective circular orbit with the following semi-major axis (Panwar and Kennewell, 1999):

$$a_{eff} = r_{perigee} + 900 \cdot (e)^{0.6} \tag{4}$$

where e is the orbit eccentricity. Day-night effects are ignored. Since this paper is mainly concerned with lifetime reduction, such effects are considered beyond the scope.

The top three lines in Fig. 2 show the nominal lifetime of the objects without any Δv. Clearly and as expected, the lifetimes of these objects depend on altitude. In Fig. 2, the horizontal line shows the 25 year guideline. The altitude below which this guideline is naturally followed is approximately 890 km for a 1 cm object, 825 km for a 5 cm object and 775 km for a 10 cm object. At higher altitudes than these values, the objects will have to be lowered artificially to satisfy the requirement. The two sets of lines below (dotted and dashed) correspond to the reduced lifetime after a change in velocity Δv of respectively 50 and 150 m/s. The lifetimes of the now elliptical orbits after a Δv are computed following Eqs. 3 and 4. Assumptions made for the computation of orbital lifetime are validated in A.

3. Single debris object results

A limited number of possible geometries exists from which the laser system can target an object: the coplanar case where both objects orbit in the same plane, and the non-coplanar case where the laser system has an azimuth angle ϕ w.r.t. the target orbit.

3.1. Head-on geometry

Fig. 3 shows the induced velocity change when the debris object and laser system encounter each other in a head-on geometry, both at 800 km. The debris objects are assumed to be spherical. The results clearly depend on the AMR of the debris object, as the 10 cm object is decelerated less than the 1 cm object. The corresponding changes in orbital lifetime of the debris objects are listed in Table 2. The 1 cm object is de-orbited within 2 days after the interaction.

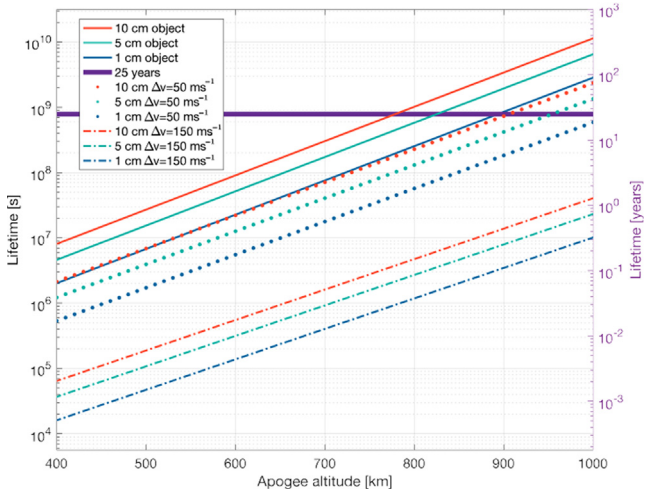

Fig. 2. Reduction of lifetime for Δv of 50 and 150 m/s on LEO debris objects.

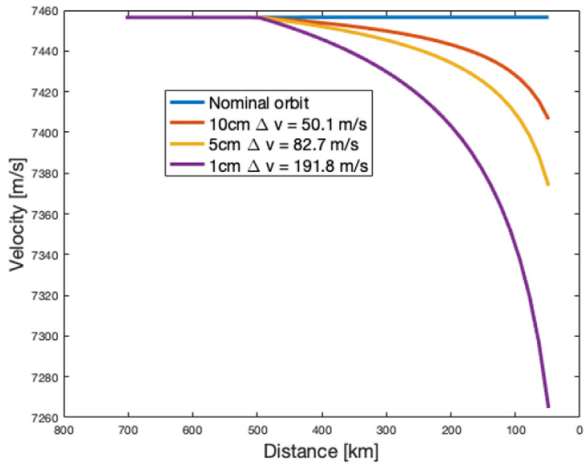

Fig. 3. Induced velocity change on objects with different size for head-on geometry at 800 km. X-axis expresses the relative distance between the debris object and the laser system during the interaction.

Table 2
Changes in lifetime of three objects after head-on encounter with laser system.

Diameter[m]	$T_{life,before}$ [yr]	$T_{life,after}$ [yr]
0.01	8.2	0.007
0.05	18.7	1.21
0.1	32.7	7.2

3.2. Non-zero azimuth angle

To get a more complete understanding of the impact of geometry, Fig. 4 shows the results when the laser system encounters 10 cm debris objects with non-zero azimuth angles. All objects initially orbit at 800 km altitude. It can be noted that the laser is less effective at high azimuth angles, as the laser then also imparts momentum in a direction normal to the debris orbit. Targeting with azimuth angle 10^o and 20^o still produces a Δv of 47 and 34 m/s respectively. The nominal lifetime of these objects was 32.7 years, but due to the laser interaction this is lowered to 8.1 and 12.8 years respectively, still a significant reduction. All objects are lowered to an orbital lifetime below the IADC guideline of 25 years.

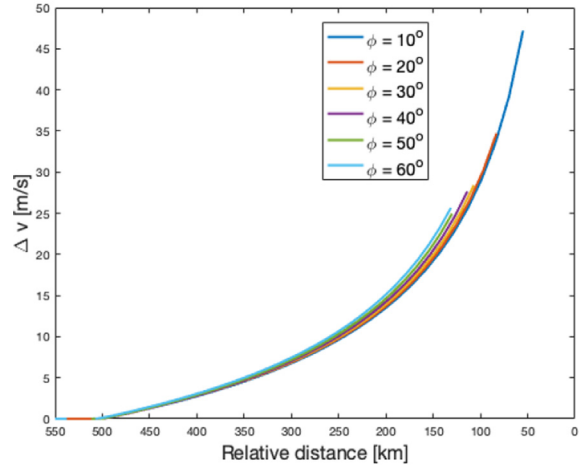

Fig. 4. Δv on 10 cm debris objects from a non-zero azimuth angle.

3.3. Different altitudes

To further assess the influence of geometry, Fig. 5 shows the induced velocity change on 10 cm debris objects when the laser system at 800 km targets them at a different altitude. The corresponding changes in orbital lifetimes can be found in Table 3. It can be noted that ablation on debris objects orbiting 200 km above or below the laser has hardly a significant effect.

The results on the objects orbiting 100 km above or below the laser are also not impressive, but for these geometries the lifetimes of the 1 cm objects may very well be lowered substantially. These results suggest an optimal performance region of about 100km above and below the laser system itself.

4. Debris population results

To get a better understanding and appreciation of the concept, the laser was tested on a debris population of 4000 objects, all created randomly within the parameter ranges listed in Table 4. The ranges are representative for the majority of small-scale debris characteristics and orbits (focusing to a large extent on Sun Synchronous Orbits).

The simulation was run for a total of 5000 interactions that occurred over a time interval of 10 days. Eclipsing effects are ignored for this simulation, since there exist SSO configurations where a spacecraft will always be illuminated by the Sun. Fig. 6 shows the lifetime reduction of every interaction after 3, 6 and 10 days. As expected,

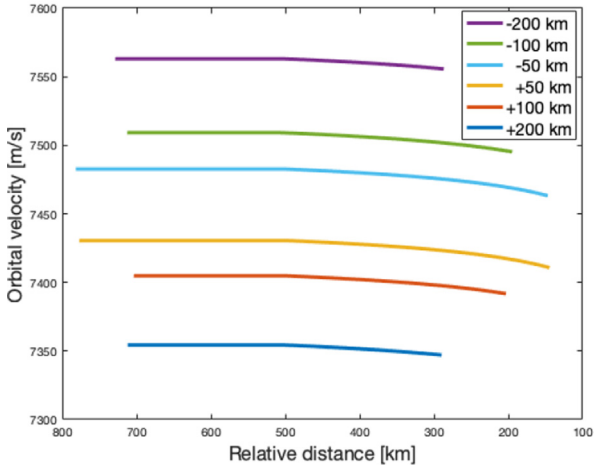

Fig. 5. Induced velocity change when the laser encounters a 10 cm object at different altitude. X-axis expresses the relative distance between the debris object and laser system during the interaction.

Table 3
Changes in velocity and lifetime when objects are at different altitudes.

h[km]	Δv [m/s]	$T_{life,before}$ [yr]	$T_{life,after}$ [yr]
600	7.9	2.9	2.6
700	15.2	9.8	7.26
750	21.6	17.9	10.8
850	21.1	60.1	36.3
900	14.3	110.23	82.3
1000	7.7	370.7	333.7

Table 4
Characteristics of simulated debris population.

Parameter	Lower limit	Upper limit
Diameter [m]	0.01	0.1
AMR [m^2/kg]	0.04	0.16
Altitude [km]	700	900
Inclination [°]	70	110

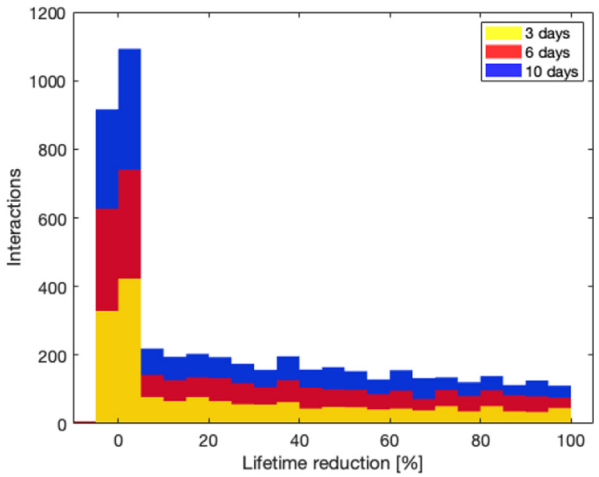

Fig. 6. Lifetime reduction for all 5000 interactions.

it can be seen that the lifetime reduction increases over time. After 10 days, a total of 4073 interactions resulted in a lifetime decrease of the targeted object. A total of 489 interactions even resulted in a lifetime reduction of more than 80%.

There are also 924 interactions that result in a slight lifetime increase. In these interactions, the geometry of the candidate debris object with respect to the laser system changes right when the system wants to start ablating the object. For example, it can be imagined that a potential candidate comes into the FOV at a relative distance of 800 km to the laser system with a high azimuth angle, yet still respecting the right conditions to be ablated. It could happen that the debris object violates one of the termination conditions during the first few seconds of ablation, after which the interaction will be stopped. In this way, these interactions are always terminated within the first few seconds of ablation and will never increase the lifetime more than about 5%. Next to this, the negative effect of these slight lifetime increases are negligible in comparison to the significant lifetime decrease that the laser produces on the debris population as a whole.

Fig. 7 shows the generated Δv plotted against the apogee of every object before the interaction. At close inspection, at the operational altitude of the laser at 800 km, a 'gap' in data points can be seen since exact head-on interactions are rare. From this altitude, the magnitude of the Δv's decrease for higher and lower debris altitude as the geometries get less and less optimal. For debris objects at $h_{apo} = 700$ km and $h_{apo} = 900$ km, still significant velocity changes of up to 90 m/s are generated. The most effective encounters correspond to objects with high AMR values.

In the 10 days of simulation time, the laser does not encounter every individual debris object. Rather, it encounters many debris objects more than once. The 5000 interactions that the laser had, were with 1739 different objects, meaning that only 43% of the population was encountered. Although this effect will be less in real life due to the much larger number of debris objects, it is still likely to happen that the laser encounters the same debris object more than once. This is because debris fragments that get a low Δv during a first interaction are likely to keep orbiting in the same region that they were in before. Next to that, debris objects from 900 km that get a moderate Δv might have their perigee lowered to the operational altitude of the laser, making a second encounter more likely.

Fig. 8 shows the lifetime of the 1739 objects before the first encounter plotted against the lifetime of the same debris objects after the last encounter. The horizontal and vertical lines depict the 25 year limit. Out of the 1739 encountered objects, there were 1479 objects with a lifetime below 25 years before the laser interaction. After the simulation, an extra 225 objects were effectively lowered below the guideline, represented by the blue dots in the bottom right of the red cross of Fig. 8. The blue dots in the top right of the cross represent the 264 objects that still have

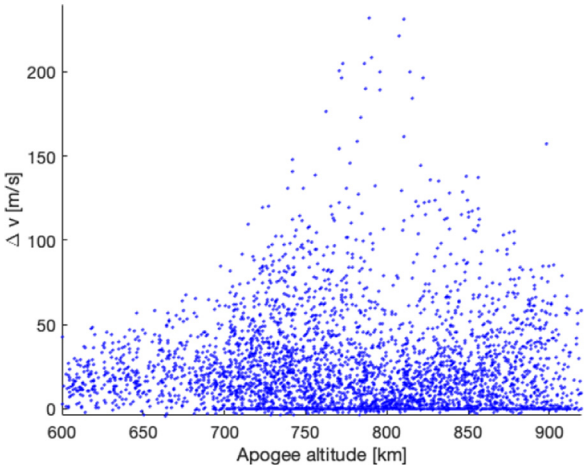

Fig. 7. Generated Δv (velocity decrease) on debris objects with different apogee altitude.

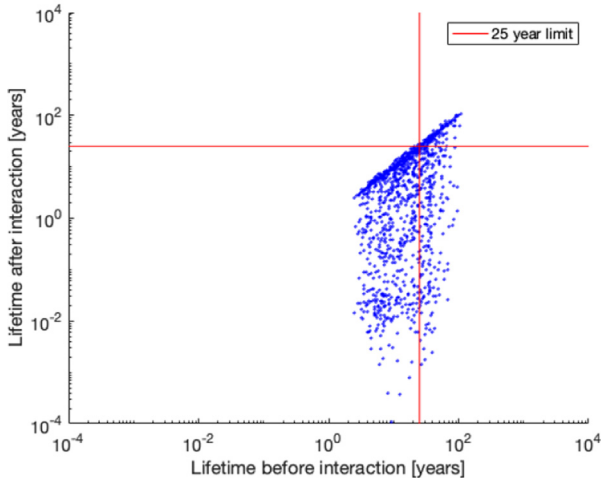

Fig. 8. Cumulative decrease in lifetime on the 1739 different encountered objects.

a lifetime of at least 25 years after the laser simulation has ended. These objects will have to be targeted again. In addition, the subset in the lower left part also benefit significantly, with major reductions in lifetime (a residual lifetime of e.g. 1 year is of course much more attractive than e.g. 24 years, although both are below the 25 year requirement).

To put the effectiveness of the system in broader perspective, the reduction to lifetimes even lower than just the 25 year guideline should be inspected as well, as these are also highly beneficial for the safety of the LEO region. Fig. 9 shows the evolution of the number of objects with a lifetime of 25 years and of 1 month, before and after the laser interaction. The longer the simulation runs, the more objects have their lifetime decreased. An object may only be called effectively lowered below a certain lifetime if its original lifetime was above this value. The large increase

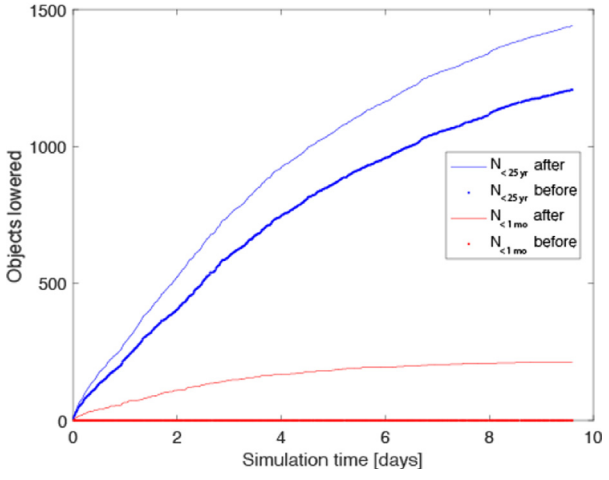

Fig. 9. Evolution in time of number of objects lowered below lifetime values.

of effectively lowered objects with lifetime below 1 month (magenta line) is due to the fact that before the interaction there were no objects with such a low lifetime.

After 4 days, the laser has already effectively lowered 169 objects to a lifetime of 1 month or less and 189 objects to less than 25 years. After 10 days this has increased to 212 objects to lifetimes below 1 month and 233 below 25 years.

4.1. Longer timescale

To predict the performance of the laser beyond 10 days, the results should be extrapolated on a longer timescale. Fig. 9 shows the evolution of the amount of debris objects that had their lifetime decreased below 25 years and below 1 month over the full simulation period of 10 days. The bold lines indicate how many objects already had a lifetime below 25 years and 1 month before the interaction. As such, the difference between the fine and bold lines express how many objects are effectively lowered. It can be seen that the evolution of the effectively lowered objects is not linear over time, but seems to stagnate after about 5 days. This is because the small population size of 4000 objects causes the time intervals between successive encounters to be unrealistically long. Near the end of the simulation the time between new interactions is about 16 min. When employed in the real LEO region, the laser system will almost constantly be able to encounter new debris objects, which increases the performance of the laser system. A more realistic value for the time between successive encounters is about 5 min. Up to day 4 of the simulation, debris objects are still being encountered within 5 min of each other, so the performance of the system up to day 4 is taken as the reference value. In this time frame, the laser effectively lowered 169 debris objects below a lifetime of 1 month (Fig. 9). Extrapolating such a removal rate to a longer timescale, a yearly number of 15 241 objects could be removed from orbit which would be an impressive achievement. This would imply the active removal of more than 150 000 debris fragments from the LEO region within 10 years, which would be a great success. These results suggest that a laser ablation system could function very efficiently as a small-scale debris removal method.

5. Conclusions

This report has researched the performance of a space-based laser system for the removal of space debris fragments between 1 and 10 cm. The designed laser system shoots 300 J energy pulses with 66.66 Hz repetition frequency using a laser wavelength $\lambda = 335$ nm and a $D = 2.0$ m mirror. With these laser settings, the fluence ablation threshold is passed at a relative distance of 500 km from the laser.

The procedure of the program was explained in detail and the termination conditions were highlighted. The system was tested for all possible geometries at which it might encounter debris objects during a real-time simulation.

The laser is tested on a simulated debris population containing 4000 debris objects with AMR between 0.04 and 0.16 m^2/kg and ranging from 700 to 900 km altitude. A 10 day simulation was run in which the laser had 5000 encounters with 1739 different objects. After 10 days the lifetime of a total of 233 objects with original lifetime higher than 25 years are lowered below the 25 years guideline and the lifetimes of 212 objects are lowered to below 1 month.

Extrapolating the values after 4 days of simulation time to a longer time period predicts that the laser could lower the lifetime of about 15 000 debris objects to below one month, per year. These results suggest that a space-based laser system could operate very well as a small-scale debris removal technique and could help ensure the future safety of the space environment.

Declaration of Competing Interest

The authors declare that they have no known competing financial interests or personal relationships that could have appeared to influence the work reported in this paper.

Appendix A. Uncertainties

Some assumptions that this paper has made should be highlighted, most of which were done to reduce the computation time. First, the atmospheric density in LEO has been simulated by an exponential atmosphere model, which drastically reduced computation time. Table 5 shows the uncertainties that this assumption brings forward.

The values are correct to around ±10%. Since the average density values of the U.S. standard atmosphere themselves have a large standard deviation resulting from the fluctuations of solar activity, the 10% error of the exponential model is considered to be a sufficiently accurate estimation.

Another assumption that produces discrepancies is the method of computing the orbital lifetime. The nominal lifetimes in this report are computed assuming that the debris object experiences a constant atmospheric drag at the initial altitude (Wertz et al., 2011). It would have been more accurate to integrate Eq. 3, including the change in atmospheric density and orbital period as the object spirals towards Earth. However, this would have substantially increased the computation time of the simulation. Table 6 shows the difference of the orbital lifetime of this report (Fig. 2) and that of Fig. 1 in (Phipps et al., 1996), both for a spherical object with an AMR of 0.075 m^2/kg. For objects at 600, 700 and 800 km, the lifetimes are fairly accurate: the errors in lifetime are below 5%. Larger errors are found at altitudes of 400, 500, 900 and 1000 km. First, these errors come from the assumption of an exponential atmosphere. However, the errors in Table 5 do not exactly coincide with the errors in lifetime listed in Table 6. Rather, the assumption of a constant atmospheric drag explains the errors in Table 6.

The atmospheric densities at 600 and 800 km altitude used in this report were about 10% higher than the true values. This denser atmosphere compensates for the assumption that the object experiences a constant drag, which makes the errors in lifetime accurate to below 5%. The density at 1000 km arising from the exponential model was ∼ 7.5% lower than the true value. This estimation, together with the assumption that the object experiences constant drag, accumulates to a larger error of 32.45% in the nominal lifetime. The most important thing is that the large errors are all positive, meaning that the computed lifetimes in this report are higher than the literature values. This suggests that the laser system will lower even more objects when a more accurate density model is implemented and the loss in altitude is integrated as the objects spiral into the atmosphere.

Table 5
Densities from exponential model versus densities from U.S. standard atmosphere true model (U.S. National Oceanic and Atmospheric Administration and U.S. Air Force, 1976).

h [km]	ρ_{true} [kg/m³]	ρ_{model} [kg/m³]	error [%]
200	$2.91 \cdot 10^{-10}$	$2.91 \cdot 10^{-10}$	0
400	$2.42 \cdot 10^{-12}$	$2.22 \cdot 10^{-12}$	−9.0
600	$1.75 \cdot 10^{-13}$	$1.93 \cdot 10^{-13}$	+10.2
800	$1.55 \cdot 10^{-14}$	$1.69 \cdot 10^{-14}$	+9.1
1 000	$1.59 \cdot 10^{-15}$	$1.47 \cdot 10^{-15}$	−7.5

Table 6
Comparing orbital lifetimes from this report (Fig. 2) with data from literature (Figure 1 from (Phipps et al., 1996)).

h [km]	T_{life} [yr]		error [%]
	this study	literature	
400	0.5	∼ 0.2	150
500	1.8	∼ 1.0	87
600	6.2	∼ 6	4.05
700	20.7	∼ 20	1.05
800	69.8	∼ 70	−0.25
900	234.8	∼ 200	17.65
1000	789.5	∼ 600	32.45

References

Anz-Meador, P., Potter, A., 1996. Density and mass distributions of orbital debris. Acta Astronaut. 38 (12), 927–936.

Klinkrad, H., 2006. Space debris: models and risk analysis. Springer-Praxis books in astronautical engineering. Springer; Published in association with Praxis Pub, Berlin; New York; Chichester; UK.

Krag, H., 2020. ESA, Annual space environment report. ESA Space Debris Office,. URL: https://www.sdo.esoc.esa.int/environment_report/Space_Environment_Report_latest.pdf.

Mason, J., Stupl, J., Marshall, W., Levit, C., 2011. Orbital debris–debris collision avoidance. Adv. Space Res. 48 (10), 1643–1655.

Panwar, R., Kennewell, J., 1999. Satellite orbit decay calculations. The Australian Space Weather Agency,. URL: http://www.sws.bom.gov.au/Category/Educational/Space$%$20Weather/Space$%$20Weather$%$20Effects/SatelliteOrbitalDecayCalculations.pdf.

Phipps, C., Albrecht, G., Friedman, H., Gavel, D., George, E., Murray, J., Ho, C., Priedhorsky, W., Michaelis, M., Reilly, J., 1996. Orion:

Clearing near-earth space debris using a 20-kw, 530-nm, earth-based, repetitively pulsed laser. Laser Part. Beams 14 (1), 1–44.

Phipps, C., Boustie, M., 2017. Laser impulse coupling measurements at 400 fs and 80 ps using the luli facility at 1057 nm wavelength. J. Appl. Phys. 122 (193103).

Phipps, C.R., 2014. LADROIT, A spaceborne ultraviolet laser system for space debris clearing. Acta Astronaut. 104 (1), 243–255. https://doi.org/10.1016/j.actaastro.2014.08.007, URL: https://linkinghub.elsevier.com/retrieve/pii/S0094576514003142.

Phipps, C.R., Bonnal, C., 2016. A spaceborne, pulsed UV laser system for re-entering or nudging LEO debris, and re-orbiting GEO debris. Acta Astronaut. 118, 224–236. https://doi.org/10.1016/j.actaastro.2015.10.005, URL: https://linkinghub.elsevier.com/retrieve/pii/S0094576515300485.

Schall, W.O., 1991. Orbital debris removal by laser radiation. Acta Astronaut. 24, 343–351.

U.S. National Oceanic and Atmospheric Administration and U.S. Air Force (1976). US standard atmosphere volume 76. National Oceanic and Atmospheric Administration.

Walker, L., Vasile, M., 2021. Mitigation of debris in leo using space-based lasers. In 72nd International Astronautical Congress. Dubai, United Arab Emirates.

Walker, L., Vasile, M., Warden, M., 2021. Feasibility of active debris mitigation using space-borne lasers. ESA Space Debris Office. Presented at 8th European Conference on Space Debris.

Wertz, J.R., Everett, D.F., Puschell, J.J., 2011. Space mission engineering: the new SMAD. Microcosm Press, Hawthorne CA.